Stable Patterns of Membrane Domains at Corrugated Substrates

Bartosz Różycki, Thomas R. Weikl, and Reinhard Lipowsky

Max Planck Institute of Colloids and Interfaces, Science Park Golm, 14424 Potsdam, Germany

Multicomponent membranes such as ternary mixtures of lipids and cholesterol can exhibit coexistence regions between two liquid phases. When such membranes adhere to a corrugated substrate, the phase separation process strongly depends on the interplay between substrate topography, bending rigidities, and line tension of the membrane domains as we show theoretically via energy minimization and Monte Carlo simulations. For sufficiently large bending rigidity contrast between the two membrane phases, the corrugated substrate truncates the phase separation process and leads to a stable pattern of membrane domains. Our theory is consistent with recent experimental observations and provides a possible control mechanism for domain patterns in biological membranes.

PACS numbers: 87.16.dt, 64.75.St

Introduction.—Biomimetic and biological membranes are two-dimensional liquids, in which the lipid molecules undergo fast lateral diffusion. In general, the interactions between the different lipid species may lead to the formation of intramembrane domains with distinct lipid composition. For giant vesicles prepared from three-component membranes, such domains can be directly observed by optical microscopy [1–5]. These experiments have confirmed the process of domain-induced budding as predicted theoretically [6]. The latter shape transformation provides direct evidence for the line tension of the domain boundaries, which was found to vary between 10^{-12} and 10^{-14} N for different compositions and temperatures [2] and must vanish at the critical demixing or consolute point of the membrane mixture [6].

The three-component membranes studied in [1–5] consisted of a saturated lipid such as sphingomyelin, an unsaturated phospholipid, and cholesterol. The same lipid mixtures were proposed to form domains in cell membranes [7,8] but direct imaging of these latter domains or "rafts" has turned out to be difficult. In contrast, it is now well established that the three-component model membranes exhibit two-phase coexistence regions in which the membrane components separate into liquid-ordered ($\mathcal{L}_o$) and liquid-disordered ($\mathcal{L}_d$) domains that are enriched in the saturated and unsaturated lipids, respectively.

The micrometer-size domains observed in three-component membranes must arise from the growth and coarsening of much smaller domains, a process which acts to reduce the line energy of the domain boundaries between the $\mathcal{L}_o$ and $\mathcal{L}_d$ domains. This coarsening process can be modified by constraints on the membrane shape as observed in recent experiments [9,10], in which the membranes adhered to a substrate surface. For a planar substrate, the membrane domains should again undergo the same coarsening process as for giant vesicles. For a corrugated substrate surface as in Fig. 1, on the other hand, the domains tend to form certain domain patterns as observed in [9,10]. One important and open question is whether

these domain patterns are metastable or represent the true equilibrium states of the membranes.

In this Letter, we will address and answer this question. First, we will clarify the basic mechanism underlying the observed domain patterns and show that these patterns arise from the competition between the line tension, λ, of the domain boundaries and the bending rigidities κ_o and κ_d of the ordered and disordered liquid phases, where we take $\kappa_o > \kappa_d$ as in [2]. The bending rigidity contrast $\Delta\kappa \equiv \kappa_o - \kappa_d$ and the line tension λ define the elastic length scale $\xi_{\text{el}} \equiv \Delta\kappa/\lambda$ which must be compared with another length scale, ξ_{to}, that is determined by the surface topography alone. If the elastic length scale ξ_{el} exceeds the topographical length scale ξ_{to}, the pattern with many striped domains is predicted to be globally stable and to represent the true equilibrium state of the membrane. For
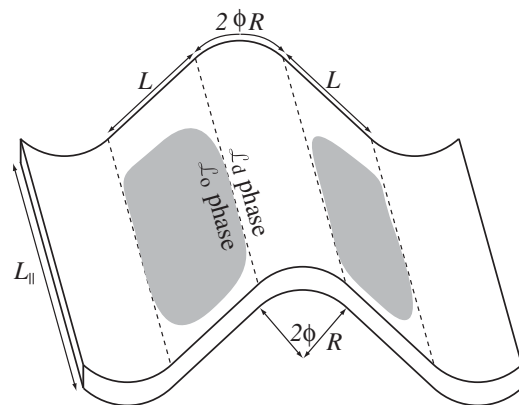

FIG. 1. Multicomponent membrane adhering to a corrugated substrate surface—In this example, the topography is periodic in one direction and characterized by the curvature radii $\pm R$ of the cylindrical ridges and valleys, the width L of the flat surface segments, and the tilt angle ϕ. The membrane contains liquid-ordered ($\mathcal{L}_o$, gray) and liquid-disordered ($\mathcal{L}_d$, white) domains. The $\mathcal{L}_o$ phase, which has a higher bending rigidity than the $\mathcal{L}_d$ phase, tends to avoid the curved membrane regions along the ridges and valleys.

$\xi_{\text{el}} < \xi_{\text{to}}$, on the other hand, the equilibrium state consists of one large $\mathcal{L}_o$ and one large $\mathcal{L}_d$ domain, both of which cover many ridges and valleys of the surface topography [11].

Our Letter is organized as follows. We first define our theoretical model in terms of the different energies of a multicomponent membrane that forms two types of intramembrane domains and adheres to a topographically structured surface. Using this model, we then determine the phase diagram both for the grand-canonical ensemble, in which the membrane is in contact with reservoirs for the different lipid molecules, and for the canonical ensemble, in which the membrane has a constant number of lipid molecules. Both phase diagrams are quantitatively confirmed by extensive Monte Carlo simulations, which provide additional insight into the anisotropic coarsening process of the membrane domains.

Theoretical model.—The system under consideration is a multicomponent lipid membrane, which strongly adheres to a topographically structured substrate as in Fig. 1. If the membrane is quenched into (or prepared within) the $\mathcal{L}_o - \mathcal{L}_d$ coexistence region, it forms two types of membrane domains corresponding to these two phases and characterized by bending rigidities κ_o and κ_d. The bending energy of the membrane is then given by $\mathcal{E}_{\text{be}} = \int_{\mathcal{L}_o} dA 2\kappa_o M^2 + \int_{\mathcal{L}_d} dA 2\kappa_d M^2$, where M denotes the mean curvature of the adhering membrane and the two surface integrals extend over the total area of the $\mathcal{L}_o$ and $\mathcal{L}_d$ domains, respectively.

The energy of the domain boundary separating the two lipid phases in the membrane is $\mathcal{E}_{\text{li}} = \int_{\partial \mathcal{L}_o} dl \lambda$, which depends on the line tension $\lambda > 0$ and the total length $\int_{\partial \mathcal{L}_o} dl$ of the domain boundaries. The competition of bending energy $\mathcal{E}_{\text{be}}$ and line tension energy $\mathcal{E}_{\text{li}}$ was first studied in [6] for multidomain vesicles. For adhering membranes as considered here, we must also include the adhesion energy of the membrane which has the form $\mathcal{E}_{\text{ad}} = -\int_{\mathcal{L}_o} dA W_o - \int_{\mathcal{L}_d} dA W_d$, where $W_o > 0$ and $W_d > 0$ denote the adhesion energy per unit area of the $\mathcal{L}_o$ and $\mathcal{L}_d$ membrane segments, respectively. Combining all three energy contributions, the total energy of the membrane conformation can be written as

$$\mathcal{E} = \int_{\mathcal{L}_o} dA (2\Delta\kappa M^2 - \Delta W) + \int_{\partial \mathcal{L}_o} dl \lambda, \qquad (1)$$

with the bending rigidity contrast $\Delta\kappa = \kappa_o - \kappa_d$ and the adhesion energy contrast $\Delta W \equiv W_o - W_d$. Note that $\Delta W > 0$ corresponds to a substrate that attracts the ordered $\mathcal{L}_o$ phase more strongly than the disordered $\mathcal{L}_d$ phase.

In the following, we will focus on the surface topography displayed in Fig. 1. In this case, the expression (1) for the total energy simplifies since the mean curvature M assumes only three distinct values: $M = 1/(2R)$ along the cylindrical ridges, $M = -1/(2R)$ along the cylindrical valleys, and $M = 0$ along the planar surface segments.

Phase diagram: Grand-canonical ensemble.—From the theoretical point of view, it is convenient to first consider the grand-canonical ensemble, in which the membrane is coupled to reservoirs for the different lipid molecules and the area fractions of the two types of membrane domains can adjust freely. In this case, minimization of the total energy $\mathcal{E}$ as given by (1) leads to three different membrane phases. In phases (I) and (II), the whole membrane segment that adheres to the substrate is in the $\mathcal{L}_d$ phase and in the $\mathcal{L}_o$ phase, respectively. In phase (III), on the other hand, the two phases separate in such a way that the membrane stripes that adhere to the flat pieces of the substrate are in the more rigid $\mathcal{L}_o$ phase whereas the membrane parts that adhere to the ridges and valleys of the substrate stay in the $\mathcal{L}_d$ phase. More precisely, the membrane attains phase (I) if

$$\frac{\phi\Delta\kappa}{\lambda R} > \left(1 + \frac{2\phi R}{L}\right)\frac{L\Delta W}{\lambda} \quad \text{and} \quad \frac{L\Delta W}{\lambda} < 2, \qquad (2)$$

phase (II) if

$$\frac{\phi\Delta\kappa}{\lambda R} < \min\left[\left(1 + \frac{2\phi R}{L}\right)\frac{L\Delta W}{\lambda}, 2 + \frac{2\phi R}{L}\frac{L\Delta W}{\lambda}\right] \qquad (3)$$

and phase (III) if

$$\frac{\phi\Delta\kappa}{\lambda R} > 2 + \frac{2\phi R}{L}\frac{L\Delta W}{\lambda} \quad \text{and} \quad \frac{L\Delta W}{\lambda} > 2. \qquad (4)$$

Inspection of the inequalities (2)–(4) shows that the overall phase diagram is determined by three dimensionless parameters as given by $\phi\Delta\kappa/\lambda R$, $L\Delta W/\lambda$, and $2\phi R/L$. The first two parameters are proportional to the bending rigidity contrast $\Delta\kappa$ and to the adhesion energy contrast ΔW, respectively, and inversely proportional to the line tension λ. The third parameter $2\phi R/L$ depends only on the topography of the substrate surface; compare Fig. 1. The phase diagram corresponding to fixed topography with $2\phi R/L = 1/3$ is displayed in Fig. 2.

The three regimes in Fig. 2 may be distinguished by the area fraction X_o of the $\mathcal{L}_o$ domains. This fraction is defined via $X_o \equiv A_o/(A_o + A_d)$, where A_o and A_d represent the total areas of the $\mathcal{L}_o$ and $\mathcal{L}_d$ domains. In regimes (I), (II), and (III), one has $X_o = 0$, $X_o = 1$, and $X_o = 1/(1 + 2\phi R/L)$, respectively, which implies first order transitions between these regimes. The three phase boundaries, which correspond to the dashed lines in Fig. 2, meet in a triple point. This point is located at $2\lambda = L\Delta W$ and $2\lambda(1 + 2\phi R/L) = \phi\Delta\kappa/R$.

Phase diagram: Canonical ensemble.—Next, let us consider an adhering membrane with a certain, fixed lipid composition. In equilibrium, the area fraction X_o of the $\mathcal{L}_o$ domains then attains a fixed value as well, and the adhesion energy contrast ΔW now plays the role of a Lagrange multiplier in (1). The corresponding phase diagram is shown in Fig. 3 as a function of area fraction X_o and dimensionless rigidity contrast $\phi\Delta\kappa/\lambda R$. The three
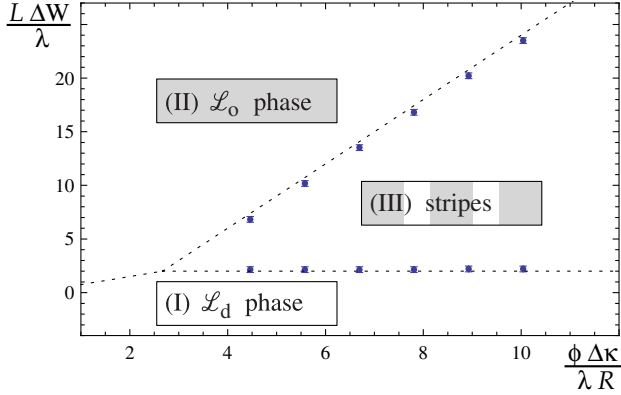
FIG. 2 (color online). Phase diagram for the grand-canonical ensemble as a function of the two dimensionless parameters $\phi\Delta\kappa/\lambda R$ and $L\Delta W/\lambda$ for $2\phi R/L = 1/3$. The dashed phase boundaries have been obtained by minimization of the total membrane energy $\mathcal{E}$ as given by (1), the data points by Monte Carlo simulations. Regimes (I) and (II) correspond to uniform membranes in the $\mathcal{L}_d$ and $\mathcal{L}_o$ phase, respectively. Regime (III) is determined by the inequalities (4) and corresponds to a striped membrane in which the membrane domains that adhere to the flat pieces of the substrate are in the more rigid $\mathcal{L}_o$ phase while the domains that adhere to the ridges and valleys stay in the $\mathcal{L}_d$ phase.

regimes (I), (II), and (III) of the grand-canonical phase diagram in Fig. 2 are mapped onto three vertical lines with constant X_o in the canonical phase diagram; see Fig. 3. The coexistence lines in the grand-canonical phase diagram, on the other hand, are now mapped into three coexistence regions of the canonical phase diagram as shown in Fig. 3.
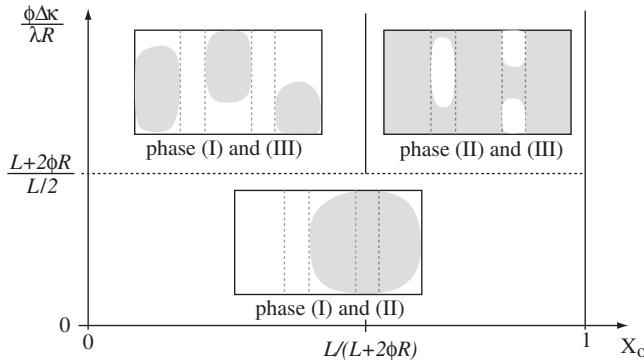

FIG. 3. Phase diagram in the canonical ensemble as a function of area fraction X_o and dimensionless rigidity contrast $\phi\Delta\kappa/\lambda R$. The three phases (I), (II), and (III) are now represented by three vertical lines with $X_o = 0$, $X_o = 1$ and $X_o = L/(2\phi R + L)$, respectively. For intermediate values of the area fraction X_o, one has coexistence regions in which two of the three phases coexist. The horizontal dotted line with $\phi\Delta\kappa/\lambda R = 2(2\phi R + L)/L$ represents transitions from a membrane with many striped domains to a membrane with two large domains.

The horizontal dotted line in Fig. 3 represents transitions from a membrane with many striped domains to a membrane with two large domains. This line is given by $\phi\Delta\kappa/\lambda R = \phi\xi_{el}/R = 2(2\phi R + L)/L$. The latter relation implies that the elastic length scale $\xi_{el} = \Delta\kappa/\lambda$ must be compared with the topographical length scale

$$\xi_{to} \equiv 2R(2\phi R + L)/(\phi L), \qquad (5)$$

which depends only on the substrate topography, see Fig. 1. For $\xi_{el} > \xi_{to}$, the bending rigidity contrast $\Delta\kappa$ dominates over the line tension λ and the membrane contains many striped $\mathcal{L}_o$ and $\mathcal{L}_d$ domains as confirmed by Monte Carlo simulations, see Fig. 4. For $\xi_{el} < \xi_{to}$, on the other hand, corresponding to large line tension and/or small bending rigidity contrast, the membrane will completely phase separate into two large domains.

Monte Carlo simulations.—The phase diagram obtained by energy minimization has been confirmed by Monte Carlo (MC) simulations. To perform such simulations, the membrane surface is divided up into square patches of side length a. This leads to a square lattice that is composed of parallel stripes of length $L_{\parallel}$. These stripes have alternating width L and $2\phi R$, compare Fig. 1, where the stripes with width $2\phi R$ correspond to the curved ridges and valleys of the substrate surface and will be denoted by $\mathcal{C}$. Each patch is labeled by a pair of integer numbers $i = (i_x, i_y)$ with $1 \leq i_x \leq N_x$ and $1 \leq i_y \leq N_y$. Periodic boundary conditions are imposed in both directions.
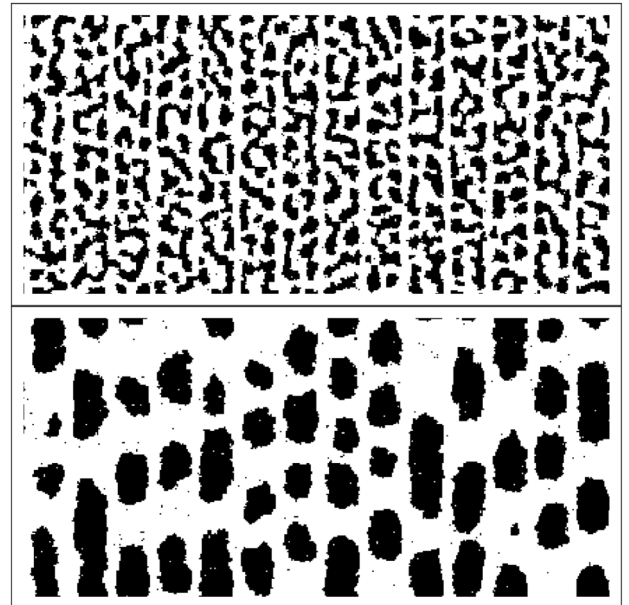

FIG. 4. Two different snapshots of membrane domains as obtained from canonical Monte Carlo simulations for area fraction $X_o = 0.4$ after (top) 10^5 and (bottom) 10^7 MC moves per patch. The black and white regions correspond to $\mathcal{L}_o$ and $\mathcal{L}_d$ patches, respectively [14].

On each patch i, we place the occupation number n_i with $n_i = 0$ and $n_i = 1$ if the square patch i is occupied by an $\mathcal{L}_d$ and an $\mathcal{L}_o$ domain, respectively. The discretized membrane energy $\mathcal{E}_{\text{dis}}$ is then given by

$$\frac{\mathcal{E}_{\text{dis}}}{a^2} = \frac{\Delta\kappa}{2R^2}\sum_{i\in\mathcal{C}} n_i - \Delta W \sum_i n_i + \frac{\lambda_0}{2a}\sum_{\langle ij\rangle} n_i(1 - n_j), \quad (6)$$

corresponding to the bending, adhesion, and line energy as in (1). The first term contains a summation over all patches i that are contained in the curvature stripes $\mathcal{C}$ while the last term contains a summation over all pairs of nearest neighbor patches $\langle ij\rangle$. The coupling constant λ_0 is related to the line tension λ via [12] $\lambda a/T = \lambda_0 a/T - \ln[(1 + e^{-\lambda_0 a/T})/(1 - e^{-\lambda_0 a/T})]$ with temperature T in energy units.

For the grand-canonical ensemble, we determined the equilibrium states of the discretized model as given by (6) using Glauber dynamics [13]. During each move of this MC algorithm, a membrane patch i is chosen randomly and the value of corresponding variable n_i is changed from 0 to 1 or from 1 to 0. This trial move is then accepted according to the Metropolis criterion. In this way, we studied the stability of different domain patterns and determined the critical nucleation size of the domains as a function of the model parameters. Discontinuous changes in the critical nucleation size of the domains indicate transitions between the homogeneous membrane phases (I) or (II) and the striped membrane phase (III). Therefore, the domain stability analysis based on the MC simulations allows us to determine the phase boundaries where parallel stripes of the $\mathcal{L}_o$ and $\mathcal{L}_d$ phase coexist in the membrane, see Fig. 2. For small lattice parameter a with $a \ll \min\{2\phi R, L\}$, our simulation results are in a good agreement with the mean field predictions (4). The MC data included in Fig. 2 were obtained for $L/a = 120$.

We also studied the process of domain formation within the canonical ensemble, in which the number $\mathcal{N} = \sum_i n_i$ of membrane patches in the $\mathcal{L}_o$ phase is kept constant. This constraint was incorporated via diffusive Kawasaki dynamics [13], in which two neighboring patches i and j with $n_i = 1$ and $n_j = 0$ are chosen randomly and the values of n_i and n_j are swapped according to the Metropolis criterion. Starting from a random initial configuration $\{n_i\}$, we then observed anisotropic coarsening processes as illustrated in Fig. 4. In this example, $\xi_{\text{el}} > \xi_{\text{to}}$ and $X_o < L/(L + 2\phi R)$ corresponding to coexistence between phases (I) and (III). As the system evolves in time, the more rigid patches start to aggregate in the flat membrane stripes and to form small domains of irregular shapes. Some of these domains shrink and, eventually, vanish whereas other domains grow and become elongated parallel to the flat membrane stripes. Since the diffusion-limited exchange process across the ridges and valleys between the flat stripes is rather slow, we performed addi-

tional simulations starting from the state of complete phase separation and confirmed that this state is stable apart from shape fluctuations of the one-dimensional interface between the coexisting phases (I) and (III).

Summary.—We have theoretically studied domain patterns in multicomponent membranes supported on corrugated substrates as in Fig. 1. We showed that the process of pattern formation is governed by the competition between bending rigidity contrast and line tension. The corresponding phase diagrams are displayed in Fig. 2 and in Fig. 3 for the grand-canonical and canonical ensemble, respectively. The stability of substrate-induced domain patterns can be understood in terms of two length scales, the elastic length $\xi_{\text{el}} = \Delta\kappa/\lambda$ and the topographical length ξ_{to} as given by (5). The substrate-induced patterns with many striped membrane domains represent the true equilibrium states of the system provided $\xi_{\text{el}} > \xi_{\text{to}}$. For the coexistence regions of the $\mathcal{L}_o$ and $\mathcal{L}_d$ phases as studied experimentally, the elastic length scale ξ_{el} is of the order of 100 nm as follows from the experimental data in [2]. This implies that both regimes $\xi_{\text{el}} > \xi_{\text{to}}$ and $\xi_{\text{el}} < \xi_{\text{to}}$ should be experimentally accessible.

[1] C. Dietrich *et al.*, Biophys. J. **80**, 1417 (2001).
[2] T. Baumgart, S. Hess, and W. W. Webb, Nature (London) **425**, 821 (2003); T. Baumgart *et al.*, Biophys. J. **89**, 1067 (2005).
[3] S. L. Veatch and S. L. Keller, Biophys. J. **85**, 3074 (2003); Phys. Rev. Lett. **94**, 148101 (2005).
[4] K. Bacia, P. Schwille, and T. Kurzchalia, Proc. Natl. Acad. Sci. U.S.A. **102**, 3272 (2005).
[5] R. Dimova *et al.*, Soft Mater. **3**, 817 (2007).
[6] R. Lipowsky, J. Phys. II (France) **2**, 1825 (1992); F. Jülicher and R. Lipowsky, Phys. Rev. Lett. **70**, 2964 (1993); R. Lipowsky *et al.*, J. Phys. Condens. Matter **17**, S2885 (2005).
[7] K. Simons and E. Ikonen, Nature (London) **387**, 569 (1997); S. Schuck and K. Simons, J. Cell Sci. **117**, 5955 (2004).
[8] S. Mukherjee and F. Maxfield, Annu. Rev. Cell Dev. Biol. **20**, 839 (2004).
[9] Tae-Young Yoon *et al.*, Nat. Mater. **5**, 281 (2006).
[10] R. Parthasarathy, Ch. Yu, and J. T. Groves, Langmuir **22**, 5095 (2006); R. Parthasarathy and J. T. Groves, Soft Mater. **3**, 24 (2007).
[11] In general, our theory applies to any coexistence region for two liquid phases within the membrane.
[12] L. Onsager, Phys. Rev. **65**, 117 (1944).
[13] K. Binder and D. W. Heermann, *Monte Carlo Simulation in Statistical Physics* (Springer-Verlag, Berlin, 1992).
[14] The snapshots shown in Fig. 4 were obtained for the following parameters: $\phi\Delta\kappa/(\lambda_0 R) = 8/3$, $2\phi R/L = 1/5$, $L/a = 25$, $\lambda_0 a/T = 1.5$ corresponding to $\lambda \simeq 0.6974\lambda_0$.